A rational Krylov subspace method for the unit cell modeling of 2D infinite periodic media

A rational Krylov subspace method for the unit cell modeling of 2D infinite periodic media

R. F. Boukadia [1,2,4], **E. Deckers** [3,4], **C. Claeys** [1,4], **M. Ichchou** [2], **W. Desmet** [1,4]
[1] KU Leuven, Department of Mechanical Engineering, Division LMSD,
Celestijnenlaan 300 - box 2420, Heverlee, Belgium

[2] École Centrale de Lyon,
36 Avenue Guy de Collongue, 69134 Ecully Cedex, France

[3] KU Leuven, Campus Diepenbeek, Department of Mechanical Engineering,
Wetenschapspark 27, 3590 Diepenbeek, Belgium

[4] DMMS lab, Flanders Make

Abstract
This paper presents a model order reduction scheme (MOR) for the forced response of 2D infinite periodic media in the Shift-Cell Operator Method framework. The proposed scheme is based on a multiparamter moment matching technique and is applied to the computation of the sound transmission loss of 2D periodic structures. To that end, a novel technique combining the Shift-Cell Operator Method and the Wave Based Method is developed, enabling the use of the proposed MOR scheme in that context. Both the new modeling technique and proposed MOR scheme are applied to a homogeneous structure and validated by comparison to the Hybrid-WFEM method. They are subsequently applied to a complex doubly stiffened panel for which good reduction factors are obtained, thus demonstrating the efficiency of the proposed modeling strategy.

1 Introduction

Owing to the impact of noise pollution on public health [1, 2], the vibroacoustic performance of panels and compact lightweight material systems is of prime importance for many applications in the automotive, aerospace, building construction and machine design industries. However, noise reduction is traditionally achieved by increasing the weight and volume of structures and vibroacoutic packages which runs contrary to technological trends and economic considerations. The tension between these two imperatives has motivated much research about so called metamaterials, often periodic in design, that exhibit sound insulation properties that go beyond the mass law. For that reason, a number of numerical methods have been developed to predict their vibroacoustics properties. Parinello's et al. [3, 4] transfer matrix method, the Hybrid-WFEM method [5, 6] and Christen et al. method [7] are all techniques enabling the prediction of the sound transmissions loss (STL) and absorption of periodic metamaterial solutions. They rely on the Wave Finite Element Method (WFEM) framework [8, 9, 10, 11] that combines finite element (FE) modeling and Floquet-Bloch theory [12, 13] to compute the response of a periodic medium to acoustic plane waves. In particular, the use of Floquet-Bloch boundary conditions at the interfaces of a unit cell (UC) of the periodic medium allows to restrict the computational domain to that single UC. This strategy can be carried over to more complex loads, e.g. diffuse acoustic fields, provided they are decomposed into plane waves first. The response to each plane wave is evaluated separately and the global response is obtained by superposition of the individual responses. The downside of that method, is that thousands of matrix inversion may be needed to compute, the diffuse field STL at a given frequency making the method ill suited to study the properties of complex UCs that require fine FE models with a high number of dofs. While reducing the number of matrix inversions required is not feasible, it is possible to reduce the computational cost of those operations by using model

order reduction. In this paper, a model order reduction (MOR) technique based on multiparameter moment matching is used in conjunction to a modified version of the Hybrid-WFEM method [5, 6] whereby the WFEM is replaced by the Shift-Cell Operator Method [14]. With this modification, the subspaces spanned by the rows of the fluid-structure coupling matrices become wavenumber invariant which both facilitate the moment matching process and is conjectured to lead to smaller Reduced Order Models (ROMs).

The rest of this paper is organised as follows. In Section 2, a brief overview of the Shift-Cell Operator Method is given along with its combination with the novel variant of the Hybrid-WFEM method. Section 3 details the multiparameter moment matching technique used and the proposed MOR scheme. Finally, the performance of the proposed scheme is evaluated in Section 4 while Section 5 summarizes the main conclusions.

2 Fluid-Structure Coupling for The Shift Cell Operator Method

In this section, the proposed variant of the Hybrid-WFEM [5, 6] is detailed. In subsection 2.1 a brief overview of the classical FEM formalism for solids is given, introducing concepts that come to use in subsections 2.2 and 2.3. In subsection 2.2, the Shift-Cell Operator Method used for the modeling of periodic structures is presented. Finally, subsection 2.3 discusses how a shift-cell based modeling can be coupled to Wave Based acoustics modeling [15].

2.1 A brief overview of the classical finite element method

We first consider the problem of linear elasticity for a displacement field u, a volume load f and density ρ on a domain Ω with Neumann boundary conditions at its boundary $\partial\Omega$:

$$\begin{cases} div(\sigma) + f = \rho\ddot{u} \; on\, \Omega \\ \sigma.\vec{n} = \sigma_0 \; on\, \partial\Omega \end{cases} \tag{1}$$

The stress tensor σ is linked to the linear strain tensor ϵ by a forth order symmetric tensor C representing Hooke's law of elasticity as per equation (2) in which Einstein's notation is used:

$$\sigma_{ij} = C_{ijkl}\epsilon_{kl} \tag{2}$$

Equation (2) is put in vector form by focusing on the 6 independent components of the strain and stress tensors. The following notations are introduced:

$$\begin{cases} \epsilon_v = [\epsilon_{11}, \epsilon_{22}, \epsilon_{33}, 2\epsilon_{23}, 2\epsilon_{13}, 2\epsilon_{12}]^T \\ \sigma_v = [\sigma_{11}, \sigma_{22}, \sigma_{33}, \sigma_{23}, \sigma_{13}, \sigma_{12}]^T \end{cases} \tag{3}$$

Leading to the vector form of equation (2):

$$\sigma_v = C_m\epsilon_v \tag{4}$$

With C_m a 6 by 6 symmetric matrix representing Hooke's law. In order to completely rewrite equation (1) in a FEM friendly way, two differential operators are introduced:

$$D = \begin{bmatrix} \frac{\partial}{\partial x} & 0 & 0 \\ 0 & \frac{\partial}{\partial y} & 0 \\ 0 & 0 & \frac{\partial}{\partial z} \\ 0 & \frac{\partial}{\partial z} & \frac{\partial}{\partial y} \\ \frac{\partial}{\partial z} & 0 & \frac{\partial}{\partial x} \\ \frac{\partial}{\partial y} & \frac{\partial}{\partial x} & 0 \end{bmatrix} \; and \; D^T = \begin{bmatrix} \frac{\partial}{\partial x} & 0 & 0 & 0 & \frac{\partial}{\partial z} & \frac{\partial}{\partial y} \\ 0 & \frac{\partial}{\partial y} & 0 & \frac{\partial}{\partial z} & 0 & \frac{\partial}{\partial x} \\ 0 & 0 & \frac{\partial}{\partial z} & \frac{\partial}{\partial y} & \frac{\partial}{\partial x} & 0 \end{bmatrix} \tag{5}$$

Because of their differential nature, these operators can only be used to left multiply when doing matrix operations. It should also be noticed that:

$$\begin{cases} \epsilon_v = Du \\ div(\sigma) = D^T \sigma_v \end{cases} \tag{6}$$

The first part of equation (1) is then rewritten as:

$$D^T C_m D u + f = \rho \ddot{u} \tag{7}$$

Introducing a vector test function w belonging to the relevant space S, the weak form of equation (7) is derived:

$$\forall w \in S,\ \iiint w^T D^T C_m D u + \iiint w^T f = \iiint w^T \rho \ddot{u} \tag{8}$$

Integrating by part and using the boundary conditions, equation (9) is derived:

$$\forall w \in S,\ \iiint w^T f + \iint w^T \sigma_0 = \iiint (Dw)^T C_m D u + \iiint w^T \rho \ddot{u} \tag{9}$$

With σ_0 defined in equation (1). Appropriate shape functions can then be chosen for w and u leading to a FEM discretatization. In most cases the same shape functions are used for w and u which leads to symmetric mass and stiffness matrices.

2.2 The Shift Cell Operator Method

The Shift Cell Operator Method [14] was invented to compute the dispersion curves of 2D periodic media in any direction, which was not possible using the WFEM. The method works mostly like FEM with a simple difference: A change of variables is operated in the displacement variable u and the equation of motion is rewritten for functions v and g such that:

$$\begin{cases} u(x,y,z,t) = v(x,y,z,t) e^{-i(k_x x + k_y y)} \\ f(x,y,z,t) = g(x,y,z,t) e^{-i(k_x x + k_y y)} \end{cases} \tag{10}$$

Equation (7) is then rewritten using v and g:

$$\begin{cases} (D_{xy}^T C_m D_{xy} v + g) e^{-i(k_x x + k_y y)} = \rho v e^{-i(k_x x + k_y y)} \\ D_{xy} = D - i k_x D_x - i k_y D_y \end{cases} \tag{11}$$

With D_x and D_y matrices, and not differential operators, defined in equation (12):

$$D_x = \begin{bmatrix} 1 & 0 & 0 \\ 0 & 0 & 0 \\ 0 & 0 & 0 \\ 0 & 0 & 0 \\ 0 & 0 & 1 \\ 0 & 1 & 0 \end{bmatrix} \quad and \quad D_y = \begin{bmatrix} 0 & 0 & 0 \\ 0 & 1 & 0 \\ 0 & 0 & 0 \\ 0 & 0 & 1 \\ 0 & 0 & 0 \\ 1 & 0 & 0 \end{bmatrix} \tag{12}$$

They account for the fact that derivatives of the product of a function with an exponential follow the pattern of equation (13):

$$\forall q \in C^1(\mathbb{R}),\ \frac{\partial}{\partial x}(q(x) e^{-i k_x x}) = \left(\frac{\partial}{\partial x} q(x) - i k_x q(x) \right) e^{-i k_x x} \tag{13}$$

Taking the weak form of equation (11), and integrating by part, equation (14) is derived:

$$\begin{aligned}\iiint w^T g + \iint w^T \sigma_0 \, e^{i(k_x x + k_y y)} = &\iiint (Dw)^T C_m Dv + \iiint w^T \rho \ddot{v} \\ &+ k_x^2 \iiint (D_x w)^T C_m D_x v + k_y^2 \iiint (D_y w)^T C_m D_y v \\ &+ k_x k_y \iiint (D_x w)^T C_m D_y v + (D_y w)^T C_m D_x v \\ &- i k_x \iiint (Dw)^T C_m D_x v - (D_x w)^T C_m Dv \\ &- i k_y \iiint (Dw)^T C_m D_y v - (D_y w)^T C_m Dv\end{aligned} \tag{14}$$

Which leads to the discretization described in equation (15).

$$(K + sC + s^2 M - ik_x L_x - ik_y L_y + k_x^2 H_{xx} + k_y^2 H_{yy} + k_x k_y H_{xy})U = D_{ss} U = F \tag{15}$$

Where K, M, and C are the classical mass, stiffness and damping matrices. The additional H and L matrices are respectively symmetric and antisymmetric and account for modulation in equation (10). The interest of this discretaization is two fold. Firstly, one can impose Floquet-Bloch boundary conditions by imposing periodicity boundary conditions and choosing values for k_x and k_y [14]. Secondly, because the load and Neumann boundary conditions needs to be multiplied by $e^{i(k_x x + k_y y)}$, a plane wave load can be made to look constant by choosing matching wavenumbers in the structure. This last property is exploited in subsection 2.3.

2.3 Hybrid coupling with the shift cell operator method

This subsection describes how to modify the Hybrid-WFEM method [5, 6] and apply it to the Shift-Cell Operator Method framework to compute the sound transmission loss of a periodic structure excited by an incident plane wave. The idea is to couple an infinite 2D periodic structure occupying the region space $0 \leq z \leq h$ to two semi-infinite acoustic domains corresponding to the regions of space $z < 0$ and $z > h$. An incident acoustic field p_i is present in the half-space $z < 0$ which by fluid-structure coupling leads to a structural response, a reflected pressure field p_r, and a transmitted field p_t in the half-space $z > h$. In order to simplify the equations, the assumption that the structure considered is weakly periodic is made. This means higher order modes in the reflected and transmitted pressure fields caused by periodic diffraction can be ignored. Thus, the acoustic fields in both half spaces take the respective forms:

$$\begin{cases} p_- = p_i e^{-i(k_x x + k_y y + k_z z)} + p_r e^{-i(k_x x + k_y y - k_z z)} \\ p_+ = p_t e^{-i(k_x x + k_y y + k_z z)} \end{cases} \tag{16}$$

The fluid-structure coupling equations are given in equation (17) and are valid on Γ_- the $z = 0$ plane and Γ_+, the $z = h$ plane:

$$\begin{cases} \dfrac{1}{\rho_f} \dfrac{\partial p}{\partial n} + \dfrac{\partial^2 u}{\partial t^2} . \vec{n} = 0 \\ \sigma . \vec{n} + p\vec{n} = 0 \end{cases} \tag{17}$$

In equation (17), ρ_f is the fluid's density, u the structural displacement, σ the stress tensor, p the fluid's pressure and $\vec{n}$, the outward normal of the solid. The first line of the equation expresses the continuity of the normal acceleration while the second lines specifies how the fluid's pressure acts as a force on the solid (Neumann boundary condition). As such, the first equation gives rise to two matrices K_{ff} and M_{fs} while the second equation only gives rise to a single coupling matrix K_{sf} as it interpreted as a boundary condition. The weak form corresponding to each matrix when discretized for the Shift-Cell-Operator Method are given

in equation (18):

$$\begin{cases} K_{ff} \leftrightarrow \dfrac{1}{\rho_f} \iint w_f^* \dfrac{\partial p}{\partial n} e^{i(k_x x + k_y)} \\ M_{fs} \leftrightarrow \iint w_f^* \dfrac{\partial^2 v}{\partial t^2} . \vec{n} \\ K_{sf} \leftrightarrow \iint (w_s \vec{n}) p e^{i(k_x x + k_y y)} \end{cases} \tag{18}$$

The shape functions for v and the usual FEM shape functions are identical to the test functions w_s while the shape functions for the pressure p are chosen according to equation (16). Finally the test functions w_f are chosen as the product of the pressure shape functions with $e^{i(k_x x + k_y y)}$. With these choices, the terms in $e^{i(k_x x + k_y)}$ vanish from both the pressure and solid the shape functions such that the matrices depend only of k_z. Specifically, K_{ff} scales with $|k_z|^2$, M_{fs} scales with $e^{ik_z z_0}$ (z_0 being the z coordinate of the interface) and K_{sf} with $e^{-ik_z z_0}$. Additionally, $K_{sf} = M_{fs}^H$ with the H exponent indicating the Hermitian transpose. Because of these properties, the subspace spanned by the columns of K_{fs} is independent of the wavenumbers k_x, k_y and k_z. This property still holds when higher order modes are added to the transmitted and reflected fields though it is less obvious. The coupled system can now be considered and takes the form:

$$\begin{bmatrix} D_{ss} & K_{sf} \\ -\omega^2 M_{sf} & K_{ff} \end{bmatrix} \begin{bmatrix} U \\ p \end{bmatrix} = \begin{bmatrix} 0 \\ F_p \end{bmatrix} \tag{19}$$

With D_{ss} the matrix of equation (15). The transmission loss $\tau(k_x, k_y, k_z, \omega)$ is computed by applying periodic boundary conditions on the structural part of equation (19) and imposing the value of the incident pressure p_i. After solving the system the transmission loss is obtained:

$$\tau(k_x, k_y, k_z, \omega) = \frac{|p_t|^2}{|p_i|^2} \tag{20}$$

The diffuse field transmission loss $\tau_d(\omega)$ can be computed by averaging the transmission loss $\tau(k_x, k_y, k_z, \omega)$ for acoustic wave coming from all incident directions. The detailed process can be found in [7, 3, 16].

3 Model Order Reduction Scheme

This section details the model order reduction scheme used in section 4. An overview of the underlying multiparameter moment matching method is given in subsection 3.1. Finally, the details of the proposed MOR algorithm are discussed in subsection 3.2.

3.1 Multiparameter moment matching

The proposed MOR method is based on the moment matching concept which seeks to match the transfer function of the full order model (FOM) by replicating the first terms of its power series around an expansion point (see equation (22)). Herein, this method is applied to the structural part of the Hybrid-Shift-Cell modeling of the transmission reflection problem and can be considered a particular case of the technique presented in [17]. The staring point is the discretized equation of motion obtained via the shift-cell operator method:

$$(K + sC + s^2 M - ik_x L_x - ik_y L_y + k_x^2 H_{xx} + k_y^2 H_{yy} + k_x k_y H_{xy}) U = F \tag{21}$$

In equation (21) s is the Laplace variable for the time domain, k_x and k_y are the wavenumbers of the shift-cell operator method, U is the structural displacement matrix and F a matrix whose columns span the subspace of inputs. A development of U into a multiparamter series is realised at the $(0, 0, 0)$ expansion point:

$$U = \sum_{(p,q,r) \in \mathbb{N}^3} U_{p,q,r} k_x^p k_y^q s^r \tag{22}$$

In order compute the moments $U_{p,q,r}$ a recurrence relationship is established between them. First, equation (21) is rewritten in a more practical form:

$$[I_n + K^{-1}(sC + s^2M - ik_xL_x - ik_yL_y + k_x^2H_{xx} + k_y^2H_{yy} + k_xk_yH_{xy})]U = (K^{-1}F) \tag{23}$$

Finally, by replacing U with the series of equation (22), the following recurrence relationship is obtained for its moments:

$$\begin{aligned} U_{p,q,r} = K^{-1}(&iL_xU_{p-1,q,r} + iL_yU_{p,q-1,r} - CU_{p,q,r-1} \\ &- H_{xx}U_{p-2,q,r} - H_{yy}U_{p,q-2,r} - MU_{p,q,r-2} - H_{xy}U_{p-1,q-1,r}) \end{aligned} \tag{24}$$

With the initial condition:

$$U_{0,0,0} = K^{-1}F \tag{25}$$

This makes it possible to match the moments of U in a classical manner. Because of the multiple parameters, the number of moments of order n, moments for which $p + q + r = n$, is equal to:

$$m_0 = \frac{(n+1)(n+2)}{2} \tag{26}$$

While the number of moments of orders inferior or equal to n is:

$$m_1 = \frac{n^3 + 6n^2 + 11n + 6}{6} \tag{27}$$

Thus, the growth is polynomial which is acceptable. However, matching the moments of U as per equation (24) may not be numerically stable as the moments of the system are computed explicitly without any orthogonalisation process [18]. An implicit and stable moment matching process is proposed in [19] but it would change the vector growth rate from $O(n^3)$ to $O(7^n)$. As such, its computational cost becomes prohibitive before instabilities appear in the proposed algorithm. It should also be noted that the above method can be applied to compute moments around another expansion point (k_x^0, k_y^0, s_0) by replacing (k_x, k_y, s) with $(k_x^0 + k_x, k_y^0 + k_y, s_0 + s)$. Hence, numerical stability issues can also be mitigated by working with multiple expansion points.

3.2 MOR strategy

The proposed MOR strategy works by producing a projection basis $P \in \mathbb{C}^n$ that spans the subspace of the moments of the displacement matrix at one or several expansion points. From the matrix P the ROM's matrices are produced via Galerkine projection:

$$\begin{cases} K^r = P^H K P \\ C^r = P^H C P \\ M^r = P^H M P \\ L_x^r = P^H L_x P \\ L_y^r = P^H L_y P \\ H_{xx}^r = P^H H_{xx} P \\ H_{xy}^r = P^H H_{xy} P \\ H_{yy}^r = P^H H_{yy} P \end{cases} \tag{28}$$

The assessment of the quality of the ROM is done via residuals as defined in equation (29) which avoids the direct computation of the FOM response:

$$\begin{cases} U_r = (K^r + sC^r + s^2M^r - ik_xL_x^r - ik_yL_y^r + k_x^2H_{xx}^r + k_y^2H_{yy}^r + k_xk_yH_{xy}^r)^{-1}(P^HF) \\ F_a = (K + sC + s^2M - ik_xL_x - ik_yL_y + k_x^2H_{xx} + k_y^2H_{yy} + k_xk_yH_{xy})(PU_r) \\ res(k_x, k_y, s) = \dfrac{\|F_a - F\|}{\|F\|} \end{cases} \tag{29}$$

The proposed algorithm iteratively produces ROMs of higher dimensions by increasing the number of moments matched and expansion points until a ROM of sufficient quality is generated. In practice, this is achieved if the residuals of all points of a validation set $\mathcal{V}_0$ are below a threshold ϵ. Both $\mathcal{V}_0$ and ϵ must be supplied by the user in addition to a decay rate $\alpha < 1$. The details of when and where new expansion points are generated are the following. At each iteration, the expansion order at all expansion points is increased. Then, a ROM is produced and an error criterion r^j is computed as per equation (30):

$$\begin{cases} r_a^j = \dfrac{1}{|\mathcal{V}_0|}\displaystyle\sum_{p\in\mathcal{V}_0} res(p) \\ r_m^j = max\{res(p),\ p \in \mathcal{V}_0\} \\ r^j = \sqrt{r_m^j r_a^j} \end{cases} \tag{30}$$

If $r^j \geq \alpha r^{j-1}$ a new expansion point is created at the point of maximal residual. Otherwise, the iterative process continues normally with increasing the order of active expansion points. The algorithm stops when $r_m^j \leq \epsilon$.

4 Numerical Results

In this section, the proposed modeling technique and model order reduction scheme are applied to two examples. First, the proposed modeling strategy is compared to the Hybrid-WFEM method and validated in subsection 4.1. It is then applied to the full 3D FEM modeling of a doubly stiffened panel previously studied in [20, 21] via asymptotic homogenisation.

4.1 Validation Case

In this subsection, both the new hybrid variant and the proposed MOR scheme are applied to a 3mm thick homogeneous aluminum plate and compared to the classical Hybrid-WFEM modeling. All numerical methods, including the WFEM and the Shift-Cell Operator Method, are implemented on Matlab. The UC of the plate is modeled using classical 3D Lagrange $Q1$ elements with 10 perfectly cubic elements in the thickness of the plate. For the MOR scheme the frequency range $[0Hz, 10000Hz]$ is considered with a maximal residual value ϵ chosen equal to 10^{-4}. After application of the periodic or Floquet-Bloch boundary conditions the original model has 32dofs. Using the proposed MOR scheme a 4 dofs model is obtained. For the diffuse field computations, 3000 polar angles are used with only 1 azimuthal angle owing to the fact that the critical frequency is within the frequency range of interest and that the structure is isotropic. The diffuse field transmission loss obtained via both methods are presented in Figure 1. Both methods are in perfect agreement which validates the implementation of the Hybrid Shift-Cell and the proposed MOR scheme.

4.2 Doubly stiffened plate

In this subsection, the novel Hybrid-Shift-Cell modeling of section 2 is combined to the MOR scheme of section 3 to analyse a doubly stiffened panel. The panel was first introduced in [20, 21] and studied via asymptotic homogenization because of the high material property contrast between its stiffeners (Aluminum)

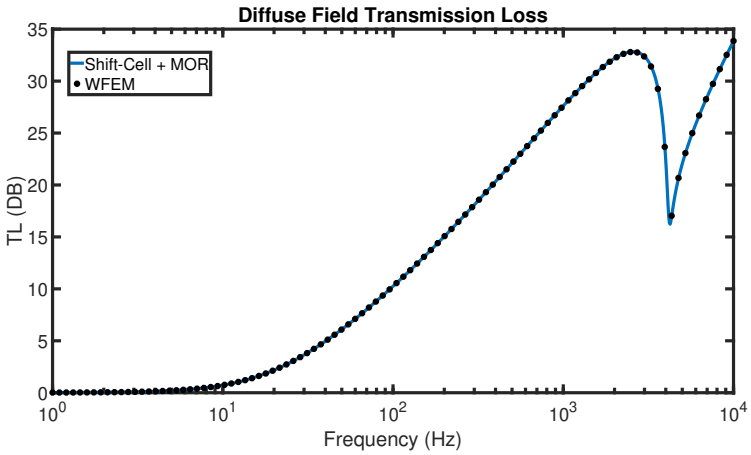

Figure 1: Diffuse field transmission loss of the aluminum plate

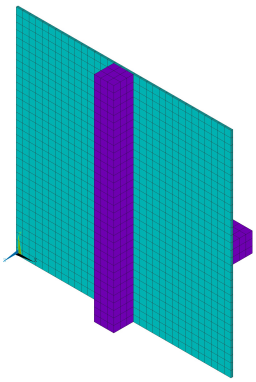

Figure 2: Mesh of the unit cell of the doubly stiffened panel. Aluminum is purple and Perspex is green

and base panel (Perspex/PPMA). This contrast leads to the appearance of full and partial resonant band-gaps for flexural and torsional waves generated by local modes of the stiffened structure. For our study, the main reason this case is considered is the fact that while the structure posses resonant band-gaps, the resonant part of the structure is also its radiating part. As such, its sound insulation properties should be non trivial. For the diffuse field computations, 500 polar angles are used with 9 azimuthal angles (since the structure is highly symmetric). Both the Shift-Cell Operator Method and of the Hybrid coupling are implemented on Matlab with standard 3D quadratic Serendipity Elements. The mesh of the structural part is presented in Figure 2. The original model had 57915 dofs and is reduced to 364 dofs using the proposed MOR scheme for a maximal residual setting ϵ of 10^{-3} on the $[0Hz, 1000Hz]$ frequency range. Hence the time needed to compute the transmission loss for one incidence angle is divided by a factor 10^4. Thanks to this, the sound transmission loss of the structure can be computed in a few hours instead of months assuming the same discretization would be used for FOM computations. The obtained diffuse field transmission loss and absorption are presented in Figure 3. Unsurprisingly, the multiple TL peaks do coincide with the band-gaps predicted in [21], however, the obtained absorption levels are rather high for a structure at that frequency range. This could be explained by the conjunction of resonance mechanism with the highly dissipative properties of perspex, effectively focusing vibration energy in the disspative part of the structure.

5 Concluding Remarks

In this paper, a novel method to evaluate the sound transmission loss of 2D infinite periodic structure was presented. The proposed method is largely based on the Hybrid-WFEM but uses the Shift-Cell Operator Method instead of the WFEM. This methodological shift renders the subspace spanned by the columns of the fluid-structure coupling matrices wavenumber invariant and enables the use of classical multiparameter

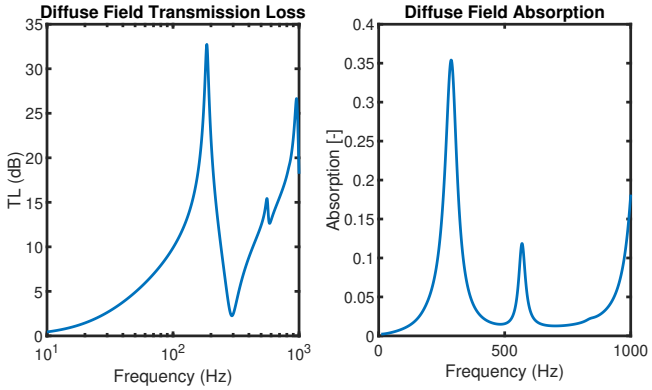

Figure 3: Transmission loss and absorption of the doubly stiffened panel

moment matching techniques to perform model order reduction. The proposed framework was validated on a simple homogeneous case and used to evaluate the STL of a complex 2D periodic structure in reasonable time. In the future, the proposed MOR scheme could also be applied to the computation of the Green's function of periodic media by using the Floquet-Bloch transform. A comparison to WFEM based modeling strategies and MOR schemes would also be valuable.

Acknowledgements

The research of R. F. Boukadia is funded by an Early Stage Researcher grant within the European Project VIPER Marie Curie Initial Training Network (GA 675441). The research of E. Deckers is funded by a grant from the Research Foundation - Flanders (FWO).

References

[1] S. A. Stansfeld and M. P. Matheson, "Noise pollution: Non-auditory effects on health," *British Medical Bulletin*, vol. 68, pp. 243–257, 2003.

[2] M. S. Hammer, T. K. Swinburn, and R. L. Neitzel, "Environmental noise pollution in the United States: Developing an effective public health response," *Environmental Health Perspectives*, vol. 122, no. 2, pp. 115–119, 2014.

[3] A. Parrinello and G. L. Ghiringhelli, "Transfer matrix representation for periodic planar media," *Journal of Sound and Vibration*, vol. 371, pp. 196–209, 2016. [Online]. Available: http://dx.doi.org/10.1016/j.jsv.2016.02.005

[4] A. Parrinello, G. L. Ghiringhelli, and N. Atalla, "Generalized Transfer Matrix Method for periodic planar media," *Journal of Sound and Vibration*, vol. 464, p. 114993, 2020. [Online]. Available: https://doi.org/10.1016/j.jsv.2019.114993

[5] Y. Yang, B. R. Mace, and M. J. Kingan, "Prediction of sound transmission through, and radiation from, panels using a wave and finite element method," *The Journal of the Acoustical Society of America*, vol. 141, no. 4, pp. 2452–2460, 2017. [Online]. Available: http://dx.doi.org/10.1121/1.4977925

[6] E. Deckers, S. Jonckheere, L. Van Belle, C. Claeys, and W. Desmet, "Prediction of transmission, reflection and absorption coefficients of periodic structures using a hybrid Wave Based – Finite Element unit cell method," *Journal of Computational Physics*, vol. 356, pp. 282–302, 2018. [Online]. Available: https://doi.org/10.1016/j.jcp.2017.12.001

[7] J.-L. Christen, M. Ichchou, A. Zine, and B. Troclet, "Wave Finite Element Formulation of the Acoustic Transmission Through Complex Infinite Plates," *Acta Acustica united with Acustica*, vol. 102, no. 6, pp. 984–991, 2016.

[8] D. J. Mead, "Free wave propagation in periodically supported, infinite beams," *Journal of Sound and Vibration*, vol. 11, no. 2, pp. 181–197, 1970.

[9] ——, "The forced vibration of one-dimensional multi-coupled periodic structures: An application to finite element analysis," *Journal of Sound and Vibration*, vol. 319, no. 1-2, pp. 282–304, 2009.

[10] J. M. Mencik and M. N. Ichchou, "Multi-mode propagation and diffusion in structures through finite elements," *European Journal of Mechanics, A/Solids*, vol. 24, no. 5, pp. 877–898, 2005.

[11] W. X. Zhong and F. W. Williams, "on the Direct Solution of Wave-Propagation for Repetitive Structures," *Journal of Sound and Vibration*, vol. 181, no. 3, pp. 485–501, 1995.

[12] G. Floquet, "Sur les équations différentielles linéaires à coefficients périodiques," *Annales scientifiques de l'École Normale Supérieure*, vol. 2e série,, pp. 47–88, 1883. [Online]. Available: http://www.numdam.org/item/ASENS_1883_2_12__47_0

[13] F. Bloch, "Über die Quantenmechanik der Elektronen in Kristallgittern," *Zeitschrift für Physik*, vol. 52, no. 7, pp. 555–600, 1929. [Online]. Available: https://doi.org/10.1007/BF01339455

[14] M. Collet, M. Ouisse, M. Ruzzene, and M. N. Ichchou, "Floquet-Bloch decomposition for the computation of dispersion of two-dimensional periodic, damped mechanical systems," *International Journal of Solids and Structures*, vol. 48, no. 20, pp. 2837–2848, 2011. [Online]. Available: http://dx.doi.org/10.1016/j.ijsolstr.2011.06.002

[15] E. Deckers, O. Atak, L. Coox, R. D'Amico, H. Devriendt, S. Jonckheere, K. Koo, B. Pluymers, D. Vandepitte, and W. Desmet, "The wave based method: An overview of 15 years of research," *Wave Motion*, vol. 51, no. 4, pp. 550–565, 2014. [Online]. Available: http://dx.doi.org/10.1016/j.wavemoti.2013.12.003

[16] R. F. Boukadia, E. Deckers, C. Claeys, M. Ichchou, and W. Desmet, "A wave-based optimization framework for 1D and 2D periodic structures," *Mechanical Systems and Signal Processing*, vol. 139, p. 106603, 2020. [Online]. Available: https://doi.org/10.1016/j.ymssp.2019.106603

[17] O. Farle, V. Hill, P. Ingelstrom, and R. Dyczij-Edlinger, "Multi-parameter polynomial order reduction of linear finite element models," *Mathematical and Computer Modelling of Dynamical Systems*, vol. 14, no. 5, pp. 421–434, 2008.

[18] P. Feldmann and R. W. Freund, "Efficient Linear Circuit Analysis by Padé Approximation via the Lanczos Process," *IEEE Transactions on Computer-Aided Design of Integrated Circuits and Systems*, vol. 14, no. 5, pp. 639–649, 1995.

[19] P. Benner and L. Feng, "A Robust Algorithm for Parametric Model Order Reduction Based on Implicit Moment Matching," *Reduced Order Methods for Modeling and Computational Reduction*, pp. 159–185, 2014.

[20] P. Fossat, C. Boutin, and M. Ichchou, "Dynamics of periodic ribbed plates with inner resonance: Analytical homogenized model and dispersion features," *International Journal of Solids and Structures*, vol. 152-153, pp. 85–103, 2018. [Online]. Available: https://doi.org/10.1016/j.ijsolstr.2018.06.012

[21] C. Boutin, P. Fossat, C. Droz, and M. Ichchou, "Dynamics of ribbed plates with inner resonance: Analytical homogenized models and experimental validation," *European Journal of Mechanics, A/Solids*, vol. 79, no. June 2019, p. 103838, 2020. [Online]. Available: https://doi.org/10.1016/j.euromechsol.2019.103838